Engineering Challenges Associated With Hydrogen Embrittlement in Steels

Kip O Findley, Colorado School of Mines, Golden, CO, United States
Samantha K Lawrence, Los Alamos National Laboratory, Los Alamos, NM, United States
Mary K O'Brien, Colorado School of Mines, Golden, CO, United States

Introduction 235
High Strength Medium Carbon Steels for Fasteners 235
Austenitic Steels for Hydrogen Gas Storage and Transportation 238
Hydrogen Induced Cracking in Pipeline Steels in Sour Service Conditions 240
Advanced High Strength Steels for Automotive Applications 242
Summary and Opportunities for Future Research and Development Directions 244
References 245

Introduction

Hydrogen embrittlement describes a phenomenon whereby the expected ductility and toughness of a material can be drastically reduced by exposure to environments that promote hydrogen ingress, resulting in catastrophic failures in service. Generally, hydrogen embrittlement requires the presence of hydrogen either pre-existing in the steel or in the environment, imposed stress on the steel (applied or residual), a susceptible microstructure, and time for hydrogen to diffuse to fracture critical locations. Johnson (1875) first observed the reduced toughness of iron in hydrochloric and sulfuric acids in 1875. Despite nearly 150 years of research into the issue of hydrogen embrittlement, the topic is still widely debated, and a number of reviews of hydrogen embrittlement of steel exist (Barrera *et al.*, 2018; Bhadeshia, 2016; Díaz *et al.*, 2016; Hirth, 1980; Oriani, 1978; Robertson *et al.*, 2015; Turnbull, 2015). These reviews are utilized in this article and a summary of the topics presented in them is provided here for reference. Both Oriani (1978) and Hirth (1980) wrote comprehensive reviews of hydrogen embrittlement of steels encompassing hydrogen solubility, equilibrium, transport, ingress into steel, and desorption from steel. Both also addressed hydrogen effects on mechanical behavior including tensile deformation and fracture. Additionally, Hirth (1980) reviewed fundamental hydrogen-dislocation interactions at various temperatures. Notably, Oriani (1978) proposed several fundamental avenues of future research, not all of which have been performed to date. Hirth (1980) reviewed various models for fracture phenomena in the presence of hydrogen. This review has since been followed by more specific reviews on particular mechanisms by Robertson *et al.* (2015) and Lynch (1988). Barrera *et al.* (2018) wrote a review on kinetics of hydrogen transport and failure mechanisms, incorporating results from studies employing computational models and simulations. Bhadeshia (2016) wrote a concise review about preventing hydrogen ingress through coatings and preventing hydrogen transport through trapping, with a specific focus on precipitation.

This article refers to multiple mechanisms of hydrogen embrittlement in the following sections. While these mechanisms are not described in detail in this article, a brief summary of key attributes is provided here along with relevant references. The observation of intergranular fracture associated with hydrogen environments and reduction in ductility has led to the theory of hydrogen enhanced decohesion (HEDE) (Gangloff, 2003; Oriani, 1978), which proposes that the cohesive strength of interfaces (i.e., grain boundaries, precipitates, inclusions, and phase interfaces) is reduced by the presence of hydrogen. Seemingly in contrast, another interpretation is that hydrogen enhances plasticity through hydrogen enhanced localized plasticity (HELP) (Birnbaum and Sofronis, 1994; Robertson, 2001) or adsorption induced dislocation emission (AIDE) (Lynch, 1988) mechanisms. Some theories have coupled mechanisms; for example, it has been suggested that HELP can increase localized plasticity at interfaces and the amount of local hydrogen, thus facilitating crack initiation by decohesion (Connolly *et al.*, 2019; Koyama *et al.*, 2014; Martin *et al.*, 2019; Novak *et al.*, 2010). Cracks may also be initiated through accumulating pressure due to hydrogen recombination to hydrogen gas at interfaces; this mechanism is theorized to be responsible for hydrogen induced cracking in pipeline steels (Findley *et al.*, 2015; Hirth, 1980; Tetelman and Robertson, 1963; Zappfe and Sims, 1941).

Building on the vast amount of work on hydrogen embrittlement, the aim of this article is to review hydrogen embrittlement mechanisms and microstructural factors that influence associated embrittlement phenomena through four application and steel product examples: medium carbon steels for high strength fasteners, austenitic steels for hydrogen gas storage and transportation, hydrogen induced cracking in pipeline steels, and advanced high strength steels. These topic areas represent a diverse and relevant range of applications where steel selection for hydrogen embrittlement resistance is critical for design.

High Strength Medium Carbon Steels for Fasteners

High strength bolts are one of the most pertinent applications associated with hydrogen embrittlement of medium carbon steels and are susceptible in multiple environments. They are often electroplated with zinc or cadmium for corrosion protection. The

electroplating process produces hydrogen, which can ingress into the steel. Furthermore, the diffusivity of hydrogen in the resulting coating is relatively low, so hydrogen can be trapped in the high strength steel (Bhadeshia, 2016; McCarty *et al.*, 1996). Thus, without a proper baking heat treatment to release hydrogen, electroplated high strength bolts are susceptible to delayed fracture when they are installed. There are many infamous examples of delayed fractures in fasteners due to this mechanism. High strength bolts are also used in offshore oil and gas environments where cathodic protection is employed to mitigate corrosion. As a result of this cathodic protection, hydrogen is generated which can ingress into the loaded bolts and cause failure (National Academy of Engineering, 2018).

High strength bolts are typically comprised of quenched and tempered martensite microstructures, which is an important class of microstructures for other applications as well, such as high strength cold rolled or hot stamped sheet steels, where hydrogen embrittlement is a concern. In general, martensite represents a high strength microstructure and therefore is naturally vulnerable to hydrogen embrittlement. There has been substantial research to investigate mechanisms of hydrogen embrittlement in martensitic microstructures and alternative high strength microstructure solutions (Asahi *et al.*, 2003; Bhadeshia, 2016; Brahimi *et al.*, 2017; Das *et al.*, 2018; Hui *et al.*, 2016; Krauss, 2011; Lee *et al.* 2016; McCarty *et al.*, 1996; McMahon, 2001; Michler and Naumann, 2010; Nagao *et al.*, 2014; Nanninga *et al.*, 2010; Wang *et al.*, 2015; Wei *et al.*, 2003, 2011; Wei and Tsuzaki, 2008). Martensitic microstructures are susceptible to hydrogen embrittlement for multiple possible reasons including a high dislocation density, on the order of 10^{14} to $10^{15}/m^2$ (De Cooman and Speer, 2011), which can serve to reversibly trap hydrogen and subsequently assist hydrogen damage processes (Hirth, 1980; Krom and Bakker, 2000; Oriani, 1978). Additionally, the presence of carbides has been proposed to assist in hydrogen assisted crack nucleation (Hirth, 1980), though some observations dispute the importance of carbides in the overall fracture process (Martin *et al.*, 2019). Finally, the prior austenite grain boundary character and presence of impurities on these boundaries may promote hydrogen embrittlement (McMahon, 2001, 2012). Fracture due to hydrogen embrittlement is typically intergranular at high strength levels but transitions to mixed intergranular and quasi-cleavage at lower strength levels (Beachem, 1972; Gangloff and Wei, 1978; Hyer-Peterson, 2019); this transition occurs approximately in the hardness range of 40–45 HRC. This observation suggests that prior austenite grain boundaries limit hydrogen embrittlement resistance at high strength levels. Both hydrogen enhanced localized plasticity and hydrogen enhanced decohesion have been proposed to contribute to hydrogen damage in these microstructures (Novak *et al.*, 2010).

With increasing tempering temperature, the strength of lath martensite generally decreases (Krauss, 2015). The susceptibility to hydrogen embrittlement correspondingly decreases, possibly due to the reduction in dislocation density and low angle grain boundary surface (at relatively high tempering temperatures). Example data from several hydrogen embrittlement studies is shown in **Fig. 1** (Brahimi *et al.*, 2017; Das *et al.*, 2018; Hyer-Peterson, 2019; Nanninga *et al.*, 2010), which demonstrates increasing hydrogen embrittlement susceptibility with increasing hardness through measurements of the reduction in notch tensile strength in hydrogen charged specimens relative to specimens tested in air. During tempering, the dislocation density decreases but the carbide volume fraction increases and transitions to primarily cementite at the higher range of tempering temperatures (in the absence of microalloying elements). As noted previously, carbides may contribute to hydrogen assisted fracture, but cementite is not thought to play a prominent role in hydrogen trapping (Bhadeshia, 2016). Thus, the trend in hydrogen embrittlement susceptibility with tempering temperature may suggest that dislocations are more important to the hydrogen embrittlement susceptibility than carbides. High strength martensite may also be vulnerable because a relatively large stress is induced for a given strain. In the presence of a notch, the amount of hydrogen has been correlated to the magnitude of the local triaxial stress (Amaro *et al.*, 2014). Therefore, for a high strength microstructure, the relatively high local stress surrounding a notch would result in larger amount of local hydrogen. The effect of notch triaxiality is apparent in the data in **Fig. 1** as the condition with the higher stress concentration factor ($k_t = 6$) has a higher reduction in notch tensile strength compared to the conditions with lower k_t.

Microstructural design strategies often involve inserting features to act as strong trap sites, inhibiting hydrogen from participating in the embrittlement process through trapping or decreased hydrogen diffusion. Most prominently, vanadium and titanium carbides have been investigated (Asahi *et al.*, 2003; Bhadeshia, 2016; Brahimi *et al.*, 2017; Lee *et al.* 2016; Oriani, 1978; Pressouyre and Bernstein, 1978; Villalobos *et al.*, 2018; Wei *et al.*, 2003, 2011), but niobium carbides and molybdenum-containing carbides (Banerjee and Chatterjee, 1999; Bhadeshia, 2016; Villalobos *et al.*, 2018, Das *et al.*, 2018; Liou *et al.*, 1993) have also exhibited the potential to increase hydrogen embrittlement resistance. There is conflicting evidence about the effectiveness of these trapping sites, which is at least partly related to the testing environment. For short term exposure or pre-charging of hydrogen through electrochemical or gaseous charging methods with limited amounts of hydrogen, the strong trap sites may tie up much of the available hydrogen and limit the hydrogen available to cause embrittlement. In contrast, when the supply of hydrogen is constant, both the strong, irreversible and reversible trap sites may saturate (Dadfarnia *et al.*, 2011), thus limiting the effectiveness of the irreversible traps and resulting in little difference in the performance of alloys with and without the strong trap sites. In some cases, it has been shown that more diffusible hydrogen is required to induce hydrogen embrittlement when microalloy precipitates are present. An example is shown in **Fig. 2(a)**, which compares notch tensile strength properties of a hydrogen charged steel similar to 4135 and a steel containing 0.6 wt% C and Mo microalloying to promote carbide formation to serve as hydrogen trapping sites (Akiyama, 2012). **Fig. 2(a)** shows fracture strength as a function of diffusible hydrogen content, where the Mo containing steel exhibits higher fracture strengths than the 4135 steel. In contrast, **Fig. 2(b)** shows notch tensile strength of the same alloys as a function of exposure time in humid environments where the Mo containing alloy has comparable notch tensile strength to the other alloy. It should be noted that the notch tensile strengths are in the upper range of data shown in **Fig. 2(a)**, but the Mo-containing alloy had a greater tensile strength in air and thus its reduction in notch tensile strength with environmental exposure

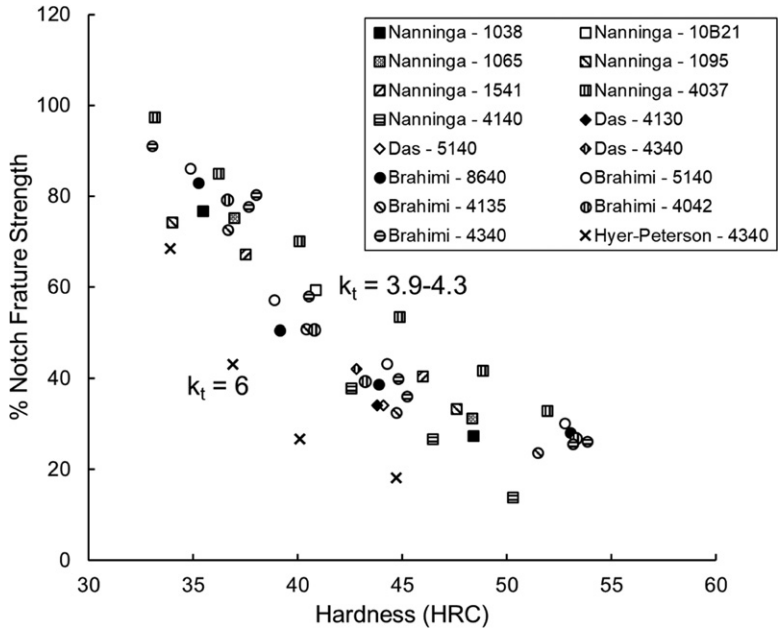

Fig. 1 Notch strength ratio, measured as the ratio of notch tensile strength in hydrogen charged specimens to the notch tensile strength of specimens tested in air. All of the conditions shown had microstructures consisting of tempered martensite. The hydrogen embrittlement tests were performed with in-situ charging while controlling either potential (− 1200 mV vs. SCE) or current density (0.1 mA/cm^2) in 3.5 pct NaCl solutions. The numbers in the legend indicate the AISI designation for the steel grade. Reproduced from Brahimi, S.V., Yue, S., Sriraman, K.R., 2017. Alloy and composition dependence of hydrogen embrittlement susceptibility in high-strength steel fasteners. Philosophical Transactions of the Royal Society A: Mathematical, Physical and Engineering Sciences 375 (2098). https://doi.org/10.1098/rsta.2016.0407. Das, T., Rajagopalan, S.K., Brahimi, S.V., Wang, X., Yue, S., 2018. A study on the susceptibility of high strength tempered martensite steels to hydrogen embrittlement (HE) based on incremental step load (ISL) testing methodology. Materials Science and Engineering A 716, 189–207. https://doi.org/10.1016/j.msea.2018.01.032. Hyer-Peterson, D., 2019. Hydrogen Embrittlement of 4340 with Martensitic and Bainitic Microstructures for Fastener Applications. (M.S. thesis). Colorado School of Mines. Nanninga, N., Grochowsi, J., Heldt, L., Rundman, K., 2010. Role of microstructure, composition and hardness in resisting hydrogen embrittlement of fastener grade steels. Corrosion Science 52 (4), 1237–1246. https://doi.org/10.1016/j.corsci.2009.12.020.

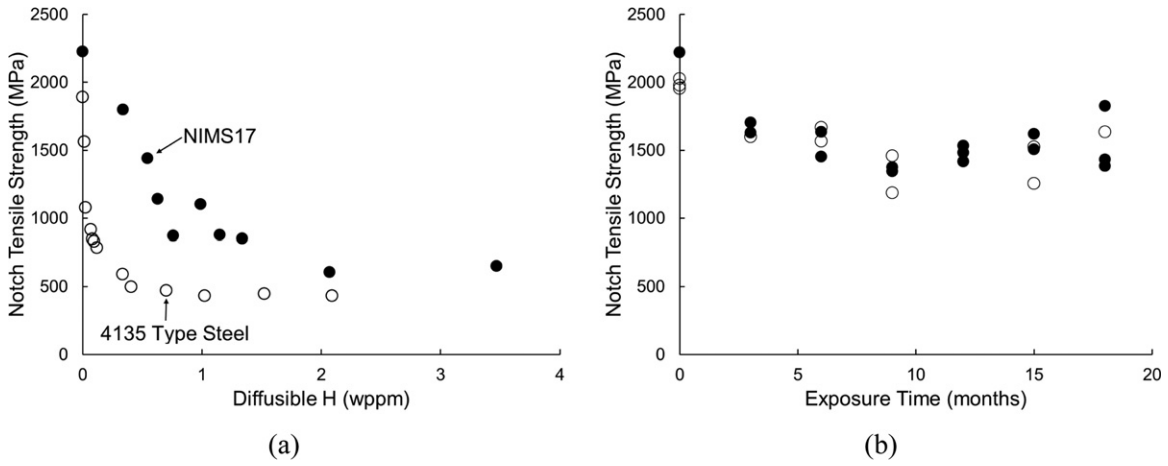

Fig. 2 (a) Notch tensile strength versus diffusible H for a steel similar to 4135 (labeled B15 in original reference) and NIMS17, designed to have 0.6 wt% C and Mo microalloying. The specimens had a notch stress concentration factor of 4.9, and slow strain rate testing was conducted after galvanostatic pre-charging and Cd plating. (b) Notch tensile strength, evaluated by slow strain rate testing, of the same alloys after long time environmental exposure in Choshi, Japan. Reproduced from Akiyama, E., 2012. Evaluation of delayed fracture property of high strength bolt steels. ISIJ International 52 (2), 307–315. https://doi.org/10.2355/isijinternational.52.307.

was higher. These data indicate that the alignment of accelerated testing methods with the service environment has to be carefully considered when evaluating hydrogen embrittlement.

Other strategies to improve hydrogen embrittlement resistance have been investigated with varying success. High strength bainite microstructures have exhibited some improvement over quenched and tempered martensite with comparable strength

levels in some studies, but the improvement is not consistent across all studies (Hyer-Peterson, 2019; Michler and Naumann, 2010; Nanninga *et al.*, 2010; Tartaglia *et al.*, 2008). Like quenched and tempered martensite, these bainitic microstructures typically contain relatively high dislocation densities, carbides at various locations in the microstructure depending on the heat treatment temperatures, and prior austenite grain boundaries. Because of these fundamental similarities in microstructure, it may be expected that differences in hydrogen embrittlement resistance are minor. It has also been suggested that high strength, drawn pearlitic microstructures may have enhanced resistance compared to other microstructures of similar strength levels, though further investigation is required (Michler and Naumann, 2010; Nanninga *et al.*, 2010); however, the use of drawn pearlite in high strength bolt applications may be limited because they likely do not have sufficient ductility for the cold-heading process necessary to manufacture bolts.

Austenitic Steels for Hydrogen Gas Storage and Transportation

Austenitic stainless steels (γ-SS) are commonly used in applications requiring good corrosion resistance or hydrogen compatibility, high ductility and toughness, and low ductile-to-brittle transition temperatures. Historically important in the petrochemical industry and gas-handling applications, 300-series stainless steels have, more recently, found extensive use in balance-of-plant (BOP) components in hydrogen storage and distribution systems (Johnson and Benard, 2016). In fact, the Japanese government currently requires the use of 316L stainless steel for all ancillary components used to construct high pressure hydrogen gas storage systems. Given that γ-SS have an extensive service history in gaseous hydrogen environments, the hydrogen effects on tensile deformation and fracture behavior of γ-SS have been extensively investigated (Caskey Jr., 1983; Hanninen, 1979; Nelson, 1983; Nibur *et al.*, 2009; San Marchi *et al.*, 2008a,b; Somerday *et al.*, 2009; Thompson and Buck, 1976). On the other hand, a more limited number of studies have focused on hydrogen effects on fatigue life (Ohmiya and Fujii, 2012, 2007) and fatigue crack growth (Kanezaki *et al.*, 2008; Skipper *et al.*, 2008) in stainless steels, even though fatigue performance is a relevant design metric for components subjected to repeated pressurization-depressurization cycles. The present review seeks to provide an overview of the current understanding of the effects of hydrogen on deformation and fracture of γ-SS during uniaxial and fatigue loading. Martensitic or ferritic stainless steels are not typically employed in high pressure gaseous hydrogen environments and are not discussed in this article, but extensive reviews on hydrogen degradation of these other high strength steel classes have been published elsewhere (Gangloff, 2003; Garrison and Moody, 2012; McMahon, 2012), and overviews of high strength steels for fasteners, steels for pipeline applications, and advanced high strength steels are provided in the other sections of this article.

Austenitic stainless steels are unique among the alloys discussed in this article, because they have a face centered cubic (FCC) crystal structure, in contrast with the primarily ferritic (body centered cubic, BCC) steels discussed in other sections. Austenite is distinguished by a comparatively low diffusivity but high solubility for hydrogen (Moody *et al.*, 1990; Turnbull and Hutchings, 1994). The most important alloying elements in γ-SS are Ni and Cr, which stabilize the austenite phase. Nitrogen is also used in solid solution to stabilize the FCC phase, and Mn is typically added to increase the solubility of N and, in some grades, as a replacement for high-cost Ni (Campbell, 2008). The microstructure of austenitic stainless steels can significantly impact their performance in hydrogen environments. Evidence suggests that subtle microstructural variations, such as compositional gradients and the presence of ferrite, may influence hydrogen-assisted fracture (Michler *et al.*, 2009; Somerday *et al.*, 2009). It can be assumed that microstructural variations may also play a role in fatigue (Ohmiya and Fujii, 2007). In addition to the primary austenite phase, several undesirable second phases can exist in γ-SS. Grain boundary carbides and δ-ferrite can precipitate during thermal exposure (Han *et al.*, 1998; San Marchi, 2012) and exacerbate corrosion susceptibility.

In this discussion, austenitic stainless steels are separated into two classes – stable and metastable – in reference to the resistance of the alloy to deformation induced phase transformation. In general, stable alloys are those that do not form α'-martensite during deformation and fracture under uniaxial tension at room temperature, such as AISI type 310, 21Cr-6Ni-9Mn, and 22Cr-13Ni-5Mn. Conversely, metastable γ-SS are those alloys that transform more readily during uniaxial deformation at room temperature, such as AISI type 304 and type 316 and their variants. Though other alloys exist in each class, those mentioned above have been extensively studied in hydrogen environments. Deformation-induced transformation in metastable alloys results in two distinct phases: hexagonal close packed (HCP) ε-martensite and body centered tetragonal (BCT) α'-martensite (Olson and Cohen, 1975). Transmission electron microscopy (TEM) investigations of metastable stainless steel suggest that one plausible transformation path involves $\gamma \rightarrow \varepsilon$-martensite nucleation by a simple faulting mechanism followed by α'-martensite nucleation at the intersection of ε bands (faults). The intersections of shear bands have been shown to be effective nucleation sites for deformation-induced α'-martensite transformation. Additionally, it is possible for α'-martensite to form at annealing twin boundaries (Caskey Jr., 1981) or directly from austenite (Lo *et al.*, 2009). Importantly, lower alloy content and lower service/test temperature promote deformation-induced martensite transformation. As noted in other sections in this article, martensite is well-established as the microconstituent in steel most susceptible to hydrogen embrittlement. However, the ultimate importance of deformation-induced martensite in the hydrogen-assisted fracture of γ-SS remains an area of active research. Reduced ductility in hydrogen environments has been attributed to α'-martensite formation (Fukuyama *et al.*, 2005; Han *et al.*, 1998; Omura *et al.*, 2007; Zhang *et al.*, 2008), but evidence for hydrogen-assisted fracture resulting from martensite transformation has not been clearly shown. Studies on hydrogen embrittlement of multiphase advanced high strength steels, which contain austenite as a secondary microconstituent, also suggest deformation induced transformation to α'-martensite degrades hydrogen embrittlement resistance as discussed later in this article.

Understanding the marked effect of hydrogen on deformation in austenitic stainless steels provides a phenomenological framework for explaining the fracture modes observed in a variety of alloys. Hydrogen facilitates dislocation motion and promotes localized deformation (Abraham and Altstetter, 1995; Birnbaum and Sofronis, 1994; Ferreira *et al.*, 1999; Liang *et al.*, 2003; Nibur *et al.*, 2006; Robertson, 2001; Sofronis *et al.*, 2001; Ulmer and Altstetter, 1991), stabilizes the edge component of mixed dislocations (Ferreira *et al.*, 1999), promoting planar slip at the expense of cross-slip, and non-uniform hydrogen concentrations induce plastic instabilities (Liang *et al.*, 2003; Sofronis *et al.*, 2001). Such non-uniform concentrations often develop in alloys prone to heterogeneous deformation, since regions of higher strain or dislocation density attract more hydrogen. Furthermore, alloys with inherent propensity for localized deformation typically experience greater loss of ductility when hydrogen charged (Nibur *et al.*, 2009), and localized deformation has been associated with a reduction in fracture resistance (Abraham and Altstetter, 1995; Ulmer and Altstetter, 1991).

Most ductile metals, including austenitic stainless steels, fracture via microvoid coalescence. Hydrogen exposure may alter the geometry and size of microvoids, thereby altering fracture resistance. For example, hydrogen can activate additional void nucleation sites, ultimately reducing dimple size. In cases where microvoid coalescence is not the predominate fracture mode, such as in austenitic stainless steel welds (Brooks *et al.*, 1983; Somerday *et al.*, 2009), hydrogen can induce fracture along interfaces. For example, hydrogen-precharged welds in the stable alloy 21Cr-6Ni-9Mn exhibit a fracture mode governed by the dendritic solidification microstructure, in which hydrogen facilitates the separation of austenite/ferrite interfaces and the fracture of the ferrite itself. Localized deformation of the austenite phase may be caused by the hydrogen-enhanced localized plasticity mechanism (Talonen and Hänninen, 2007), leading to stress concentrations at locations where deformation bands impinge on austenite/ferrite interfaces. High local stresses at the interface result in a lower remote stress for initiating cleavage cracking in ferrite (Somerday *et al.*, 2009). Similarly, fracture of a hydrogen precharged, nominally single phase 21–6–9 alloy was also determined to be governed by localized deformation (Nibur *et al.*, 2009). Deformation bands were observed to impinge on obstacles such as annealing twin boundaries or ferrite stringers, which caused stress concentrations at these sites, ultimately leading to void or microcrack formation.

Alloy content and service temperature are of paramount importance to the deformation and fracture behavior of both stable and metastable austenitic stainless steels. One metric that relates alloy composition to hydrogen degradation susceptibility is intrinsic stacking fault energy (SFE). Gibbs *et al.* (2020) have shown that austenitic stainless steels with a variety of compositions display higher sensitivity to hydrogen degradation of tensile ductility when the SFE is between 20 mJ m^2 to 40 mJ m^2. This regime also corresponds to alloys that have an increasing propensity for planar slip with decreasing stacking fault energy. Hydrogen-promoted slip planarity results in strain localization on a reduced number of slip planes (Birnbaum and Sofronis, 1994), thereby exacerbating hydrogen-assisted fracture. The service or test temperature also influences the effects of hydrogen. Tensile ductility reaches a minimum around 200K (Caskey Jr., 1983; Fukuyama *et al.*, 2005), but then begins to increase again at temperatures below 200K. This effect is attributed to limited hydrogen diffusivity at extremely low temperatures. For the same reason, the ductility trough is also governed by strain rate, i.e., for slower strain rates, there is more time for hydrogen diffusion to affect the fracture process. In general, parameters that enhance localized deformation exacerbate the effect of hydrogen on fracture behavior of austenitic stainless steels. Additionally, strength is an important consideration for the effects of hydrogen on mechanical properties of γ-SS. Annealed γ-SS have been the focus of several efforts to characterize the effects of hydrogen on tensile properties; only a few investigations have evaluated strain-hardened γ-SS. In general, hydrogen embrittlement susceptibility of strain hardened alloys is insensitive to strength in tensile tests (San Marchi *et al.*, 2008a,b) and fatigue tests (Ohmiya and Fujii, 2012; Skipper *et al.*, 2008), but a strength dependence of crack propagation in gaseous hydrogen has been observed (Perra and Stoltz, 1980).

The effect of hydrogen on fatigue resistance is an important consideration in developing design metrics for hydrogen storage and transportation infrastructure. Components in hydrogen containment systems are subjected to a significant number of pressurization-depressurization cycles over the course of system life. As with deformation and fracture, the effects of alloy and microstructure, strength, and test/service conditions on hydrogen-assisted fatigue of γ-SS are areas of active research (Aoki *et al.*, 2005; Doig, 1981; Fukuyama *et al.*, 2005; Gibbs *et al.*, 2016; Kanezaki *et al.*, 2008, 2004; San Marchi and Somerday, 2011; Michler *et al.*, 2013a,b; Nagumo *et al.*, 2003; Ohmiya and Fujii, 2012, 2007; Omura *et al.*, 2007; Skipper *et al.*, 2008; Murakami and Matsunaga, 2006). A variety of specimen geometries have been used to assess stress-controlled fatigue-life (stress-life) (Gibbs *et al.*, 2016; Kanezaki *et al.*, 2008; Michler *et al.*, 2013a,b; Murakami *et al.*, 2010; Nibur *et al.*, 2017; San Marchi *et al.*, 2012) of γ-SS in hydrogen gas. Several studies have compared stress-life as a function of alloy composition and strength, as well as test environment, by employing circumferentially notched tension (CNT) specimens under constant load amplitude in tension-tension fatigue to simulate the stress cycle experienced by pressurized components in hydrogen systems (Gibbs *et al.*, 2016; Nibur *et al.*, 2017; San Marchi *et al.*, 2012). As shown in **Fig. 3**, fatigue life of strain-hardened 316L and strain-hardened 21Cr-6Ni-9Mn was reduced by both internal hydrogen (from pre-charging) and external hydrogen (from testing in high pressure gas). Normalizing the maximum stress by the hydrogen-dependent yield strength can account for the local stress environment; doing so aligns data from tests with internal hydrogen and external hydrogen in a single band below the as-received fatigue life for 316L and aligns internal hydrogen and 103 MPa external hydrogen data for 21Cr-6Ni-9Mn, while tests conducted in 10 MPa external hydrogen remain aligned with the as-received condition (**Fig. 3(b)**) (Gibbs *et al.*, 2016). One possible explanation for the variation in fatigue performance with alloy composition and external hydrogen gas pressure is the effect of deformation-induced martensite formation. As a metastable alloy, 316L can undergo deformation-induced martensite formation during fatigue loading; α' martensite has been shown to interact with hydrogen adjacent to fatigue cracks (Fukuyama

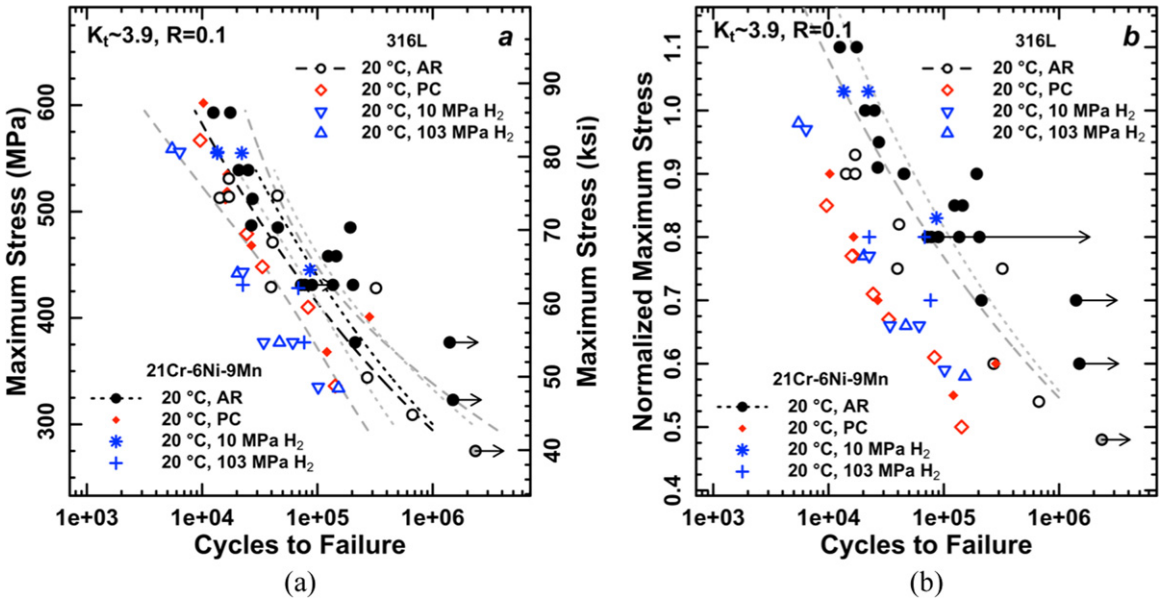

Fig. 3 Stress-life data for a metastable, strain-hardened 316L stainless steel and a stable 21Cr-6Ni-9Mn stainless steel from CNT specimens loaded in tension-tension fatigue in the as-received (AR) condition, after pre-charging (PC) to contain internal hydrogen, and during testing in external hydrogen gas at 10 MPa and 103 MPa (a). When maximum stress is normalized by hydrogen-dependent yield strength (b), stress-life data for 316L tested with internal hydrogen and in external hydrogen fall into a single band below the as-received data, while internal hydrogen and high-pressure external hydrogen stress-life data similarly align in a single band below as-received values for 21Cr-6Ni-9Mn. Data reproduced from Gibbs, P.J., Marchi, C.S., Nibur, K.A., Tang, X., 2016. Comparison of internal and external hydrogen on fatigue-life of austenitic stainless steels. In: Proceedings of the Pressure Vessels and Piping Division (Publication) PVP, 6B-2016. American Society of Mechanical Engineers. doi:10.1115/PVP2016-63563. Nibur, K.A., Gibbs, P.J., Foulk, J.W., San Marchi, C., 2017. Notched fatigue of austenitic alloys in gaseous hydrogen. In: Proceedings of the ASME Pressure Vessels and Piping Conference. pp. 459–465.

et al., 1985; Han *et al.*, 1998; Murakami *et al.*, 2010). Conversely, 21Cr-6Ni-9Mn does not form α' martensite during deformation, therefore, this microstructural feature does not play a role in hydrogen-deformation interactions. Fatigue crack growth rate (FCGR) testing also reveals some dependence of fatigue performance on alloy composition, specifically Ni content. For example, Ohmiya and Fujii (2012) investigated FCGR of SUS316-based steels with Ni contents between 9.8 mass% and 11.7 mass%; they observed a decrease in FCGR for compact tension specimens tested in high pressure hydrogen gas at room temperature as Ni content increases. Similarly, for two premium grade 316 and 316L steels (i.e., >12% Ni), fatigue crack growth rates measured in high pressure hydrogen were commensurate with those measured in laboratory air (San Marchi and Somerday, 2011). Fatigue performance of 316-based alloys in hydrogen is improved with increasing Ni content. Given the increasing cost of high Ni alloys, identifying promising alloying strategies to address performance requirements for stainless steels in hydrogen service is a vibrant research topic.

Hydrogen Induced Cracking in Pipeline Steels in Sour Service Conditions

Hydrogen embrittlement in oil and gas applications often takes the form of surface blisters and internal cracking that can lead to catastrophic failures. This phenomenon is known as hydrogen induced cracking (HIC) and generally occurs in environments with relatively high levels of hydrogen sulfide gas such as in "sour" service applications. Other names used to describe internal cracking in pipeline environments are sulfide stress cracking (SSC) and stress-oriented hydrogen induced cracking (SOHIC). However, the term HIC specifically refers to situations in which cracking occurs when no externally applied stress is required, and the presence of sulfur prevents recombination of atomic hydrogen, allowing for additional hydrogen ingress.

The HIC susceptibility of a steel can be assessed using several different testing methods. The industry standard is to use the NACE TM0284 test, which involves submersing samples in a specified aggressive solution containing a minimum partial pressure of hydrogen sulfide gas (>0.1 bar) for 96 h (NACE International, 2003). The samples are then sectioned to analyze crack lengths, thicknesses, and area relative to the total surface area. Although the NACE test is the industry standard, there are safety concerns involved with hydrogen sulfide gas, so electrochemical charging of hydrogen is sometimes used for research purposes instead (Angus *et al.*, 2014; Kim *et al.*, 2008b; Mohtadi-Bonab *et al.*, 2015; Rath and Bernstein, 1971; Venegas *et al.*, 2011; Yu *et al.*, 1997; Zakroczymski, 1985). Nearly all laboratory scale tests, including the NACE TM0284 test, use more aggressive environments than would be found in service, so the concept of using fit for service testing has been explored by several researchers but has yet to become standard industrial practice (Hay, 2001; Krom *et al.*, 1997).

Steels used for sour service oil and gas applications are low carbon, micro alloyed, and thermo-mechanically processed (TMP) (Villalobos *et al.*, 2018). Pipeline steels are generally low carbon (less than 0.1 wt pct) with solid solution strengthening elements such as Mn, Cr, and Mo, while keeping carbon equivalencies low enough for weldability concerns (De Cooman and Speer, 2011). Typical TMP regimes for pipeline steels involve a rough rolling reduction above the temperature for no recrystallization (T_{NR}) and finish rolling below T_{NR} to produce deformed austenite grains and achieve grain size refinement through austenite grain boundary pinning by microalloy precipitates. Finish rolling is followed either by air cooling or an accelerated cooling step ($\sim$18°C/s), followed by air cooling. Air cooled steels typically contain a mixture of ferrite and pearlite, while accelerated and then air cooled steels consist of non-equiaxed ferrite and secondary martensite/austenite (M/A) microconstituents. Strength is usually considered the benchmark by which a steel would be considered for sour service, as it is generally assumed that HIC susceptibility increases with increasing strength. NACE MR0175/ISO 15156 suggests a maximum yield strength of 800 MPa ($\sim$248 HV) for sour service pipeline steels (NACE International, 2003), but in practice much lower yield strengths ($\sim$400 MPa) are presently used in sour service applications.

Advances in alloy design and processing have improved HIC resistance in many modern pipeline steel alloys. Elongated manganese sulfide (MnS) stringers are particularly deleterious to HIC (Brown and Jones, 1984; Domizzi *et al.*, 2001; Huang *et al.*, 2017), so calcium has been added to reduce the aspect ratio of MnS stringers, and sulfur has been reduced to prevent extensive MnS formation (Nieto *et al.*, 2013). Oxides formed by aluminum and calcium have also been observed along crack paths, but are not nearly as prevalent as MnS stringers (Dong *et al.*, 2009; Kim *et al.*, 2008b). Moreover, copper additions have been shown to increase HIC resistance in hydrogen sulfide bearing sea water solutions through the formation of a passive layer (Inagaki *et al.*, 1978; Liou *et al.*, 1993). It should be noted that the addition of Cu has not been proven effective in either electrochemical charging experiments or solutions containing acetic acid and H_2S gas.

Despite continual improvements in steelmaking and cleanliness practices, higher strength steels are still generally more susceptible to HIC, so identifying microstructural variables that increase susceptibility will contribute to the development of higher strength steels for sour service. Microstructural parameters that may affect HIC include banding along the rolling direction, hard secondary microconstituents such as M/A, phase and interphase boundaries, rolling textures, dislocation density, and precipitates.

The M/A constituents in higher strength pipeline steels, which increase in area fraction with higher carbon contents and accelerated cooling steps, are often associated with increased HIC susceptibility (Huang *et al.*, 2011, 2017; Park *et al.*, 2008). A secondary electron micrograph of an X65 pipeline steel etched with 2 pct nital and HIC tested per NACE TM0284 is shown in **Fig. 4**. The light-colored constituents in **Fig. 4** are M/A, and the dark gray surrounding matrix is ferrite. The crack appears to propagate preferentially in the region dense in M/A constituents rather than in the ferritic matrix, which is a common observation in literature. It has been postulated that cracks propagate through the interface between M/A and surrounding ferrite, possibly with the assistance of a HEDE mechanism or by internal pressure as hydrogen becomes trapped at the M/A interface, builds to some threshold stress intensity, and a crack initiates (Findley *et al.*, 2015). As discussed in the section on Advanced High Strength Steels, M/A cracking might also be due to the high dislocation density in the martensite and retained austenite in M/A, which could act as hydrogen reservoirs for an advancing crack front. Alternatively, the increased solubility of hydrogen in austenite could result in a large concentration of hydrogen that is released upon deformation induced transformation to martensite in the plastic zone of an advancing crack front. In contrast, some studies have shown that HIC does not always occur preferentially in regions with a high M/A volume fraction (Matsumoto *et al.*, 1986; Revie *et al.*, 1993), indicating there are other relevant microstructural factors related to HIC resistance.

Segregation of alloying elements and rolling textures produced during the continuous casting process may also affect HIC resistance. Segregation of elements such as Mn and C during the continuous casting process can result in "bands" of hard constituents such as M/A or cementite in pearlite. Banding generally occurs parallel to the rolling plane through the thickness of the plate. Centerline segregation also leads to a band of high hardness at the center thickness of a plate. HIC is often observed along microstructural bands and at the centerline of pipeline steels (Domizzi *et al.*, 2001; Matsumoto *et al.*, 1986; Revie *et al.*, 1993);

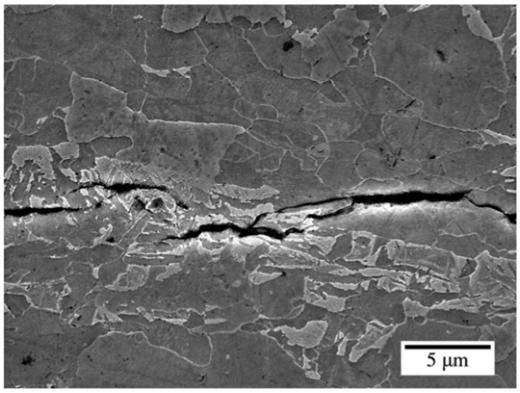

Fig. 4 Secondary electron micrograph of an X65 pipeline steel etched with 2 pct nital demonstrating cracking through a region with a high area fraction of M/A (light colored constituents). Cracking was induced by submersion in an acetic solution with H_2S gas per NACE TM0284.

however, Domizzi *et al.* suggest that banding is deleterious only if the hardness in the bands exceeds 300 HV (Domizzi *et al.*, 2001). Multiple studies have investigated the effect of rolling texture and grain boundary texture on transgranular and intergranular HIC (Mohtadi-Bonab *et al.*, 2016, 2015; O'Brien *et al.*, 2018; Venegas *et al.*, 2011; Wang *et al.*, 2009). There is some indication that {100} cleavage planes parallel to the rolling plane are detrimental to HIC, though HIC often occurs intergranularly. Studies on grain boundary misorientation and texture have not found consistent correlations between grain boundary texture and HIC resistance. Thus, there is further opportunity to characterize texture effects on HIC resistance, though there may be limited opportunities to control texture through thermomechanical processing.

Several microalloying elements such as niobium, vanadium, and titanium are employed in pipeline steels to pin austenite grains during the finish rolling step of TMP. Austenite pinning, and subsequent ferrite refinement, is achieved through the formation of small-scale carbide and/or nitride precipitates during the TMP process. In turn, precipitates can also act as either reversible or irreversible hydrogen traps, depending on the binding energy of hydrogen to the precipitate interface (Hong and Lee, 1983a; Lee and Lee, 1984; Wei *et al.*, 2011; Wei and Tsuzaki, 2008). Similar to the medium carbon steel research, much debate exists as to whether or not precipitates acting as irreversible trap sites help mitigate HIC by rendering significant fractions of the total hydrogen innocuous at ambient temperatures (Krom and Bakker, 2000; Pressouyre and Bernstein, 1978; Stevens and Bernstein, 1989; Wei *et al.*, 2011). Their effectiveness may depend on whether there is a continuous or intermittent supply of hydrogen in the system.

Cementite is also present in pipeline steels in pearlite in lower strength alloys or sometimes as intragranular precipitates, though elevated Si levels in these steels slow cementite formation. The role of cementite in hydrogen diffusion, trapping, and subsequent cracking is not clearly established. The binding energy of cementite/ferrite interfaces has been measured to range from 8 to 16 kJ mol^{-1}; these values are in the reversible trapping range (Hong and Lee, 1983a,b). As such, Johnson and Benard (2016) suggest that reversible trapping at cementite interfaces might slow diffusivity of hydrogen. In contrast, Bott *et al.* (1993) assert that the semicontinuous cementite/ferrite interfaces present in pearlite bands could allow for fast hydrogen diffusion paths. This interpretation is consistent with enhanced HIC in banded microstructures as noted previously.

Advanced High Strength Steels for Automotive Applications

In automotive lightweighting efforts, steel design has focused on enhanced combinations of strength and ductility through development of advanced high strength steels (AHSS). For these higher strength grades, there is increased concern about the possible vulnerability of these steels to hydrogen embrittlement. Further, the AHSS class includes a wide variety of alloying and microstructural approaches, and thus a large potential range of hydrogen embrittlement susceptibility. The most common AHSS approaches are dual phase (DP), transformation induced plasticity (TRIP), complex phase (CP), and martensitic steels (cold-rolled and press-hardened) and are generally defined to have ultimate tensile strengths greater than 600 MPa (De Cooman and Speer, 2011). Other approaches include quenched and partitioning (Q&P), TRIP-aided bainitic ferrite (TBF), and twinning induced plasticity (TWIP) steels.

AHSS are exposed to hydrogen during processing and in service. During steel production and vehicle manufacturing, AHSS can pick up hydrogen during pickling, zinc coating processes, spot welding, and e-coating (Bergmann *et al.*, 2018; Cornette *et al.*, 2014). The e-coating, or electro-coating process, potentially leads to the most absorption of hydrogen. During the e-coating process, steel parts are typically pre-treated in a phosphate bath. Then, the parts are submerged in an e-coat bath imposing a negative potential on the steel to attract the positively charged paint to the steel surface. As both Cornette *et al.* (2014) and Bergmann *et al.* (2018) showed, the most hydrogen absorption occurs during the phosphate pre-treatment. Both studies indicate the amount of diffusible hydrogen can reach levels of 0.2–0.25 ppm after phosphating; a study by Lovicu *et al.* (2013) found similar amounts. While this amount of diffusible hydrogen is relatively low, it can lead to reduction in mechanical performance, particularly in higher strength grades (Bergmann *et al.*, 2018). Spot welding can also promote hydrogen absorption, degrading mechanical performance (Bergmann *et al.*, 2018).

During service, steel components can pick up hydrogen due to corrosive processes, which result in the reduction of H^+ or H_2O as one of the cathodic reactions. While painting or Zn coating can protect steel from corrosive environments, breaks in the coating produce local cathodic environments (Atrens *et al.*, 2018). In an innovative study, Ootsuka *et al.* (2015) attached Devanathan-Stachurski cells, employing a bare cold-rolled steel, to vehicles driven in various conditions over a period of several days. The study concluded that hydrogen absorption did not occur until corrosion was visually observable, and both corrosion and hydrogen absorption occurred after driving on wet road surfaces for several days. Further, when a NaCl solution was sprayed on the cells before driving, both corrosion and hydrogen absorption were accelerated. However, the actual amount of hydrogen pick up may be relatively small. Cornette *et al.* (2014) utilized thermal desorption analysis to show the amount of diffusible hydrogen was less than 0.1 ppm after laboratory cyclic corrosion and salt spray tests conducted over the course of several days.

Several testing methodologies have been employed to evaluate the hydrogen embrittlement resistance of AHSS. Some methodologies utilize aggressive accelerated tests to rank relative susceptibility, while others simulate processing or service conditions with various degrees of test acceleration. Some more common types of hydrogen embrittlement testing for sheet steels are listed in **Table 1** (Atrens *et al.*, 2018; Hickel *et al.*, 2015).

One of the simplest tests to perform is electrochemical pre-charging of hydrogen into a tensile specimen followed by a constant extension rate test at quasi-static engineering strain rates typically on the order of 10^{-5} to 10^{-4}/s. The severity of charging varies with applied current density or potential, solution acidity, and time of exposure. There is variation in all of these parameters in literature studies as there is not a well-adhered to standard. However, many studies employ a 0.5 M H_2SO_4 bath with applied

Table 1 Common test methodologies, performance metrics, and hydrogen charging methods to evaluate hydrogen embrittlement susceptibility of AHSS

Test type	*Primary performance metrics*	*Hydrogen charging methods*
Constant extension rate/slow strain rate in tension/bending	Reduction in tensile ductility	In-situ or pre-charging with electrochemical Charging (e.g., H_2SO_4 or NaOH solution) often with hydrogen recombination inhibitor (e.g., Thiourea or As_2O_3)
Notch tensile testing	Reduction in notch fracture strength	Same as above
Constant load in tension/bending with notched or non-notched specimens	Time to fracture and threshold stress for fracture	Same as above
Formability test (e.g., U-Bend or Drawn Cup)	Minimum forming strain or parameter (e.g., bending radius) without fracture in defined time	Immersion (e.g., NaCl solution), hydrogen gas charging

Note: Atrens, A., Liu, Q., Zhou, Q., Venezuela, J., Zhang, M., 2018. Evaluation of automobile service performance using laboratory testing. Materials Science and Technology 34 (15), 1893–1909. doi:10.1080/02670836.2018.1495903. Hickel, T.,Nazarov, R., McEniry, E., *et al.*, 2015. Hydrogen Sensitivity of Different Advanced High Strength Microstructures (HYDRAMICROS). Publications Office of the EU.

current densities of approximately 2–10 mA/cm^2, though some studies utilize up to 30 mA/cm^2. The equivalent potential is approximately -1.0 to -1.2 V versus a reference electrode. Charging is typically performed from 30 min to 2 h (Bollinger *et al.*, 2019; Depover *et al.*, 2014; Hilditch *et al.*, 2003; Liu *et al.*, 2016, 2017; Rehrl *et al.*, 2014a,b; Ronevich *et al.*, 2010; Sojka *et al.*, 2011; Todoshchenko *et al.*, 2014; Venezuela *et al.*, 2016; Wang *et al.*, 2018; Yang *et al.*, 2016, 2018; Zhu *et al.*, 2014). **Fig. 5** shows reduction in tensile ductility ($\frac{Elongation\ in\ air - Elongation(H-Charged)}{Elongation\ in\ air} \times 100$) as a function of ultimate tensile strength for several studies employing this electrochemical charging approach; tensile ductility loss was measured as elongation loss or reduction in area loss in hydrogen charged specimens (Bollinger *et al.*, 2019; Depover *et al.*, 2014; Hilditch *et al.*, 2003; Liu *et al.*, 2016, 2017; Rehrl *et al.*, 2014a,b; Ronevich *et al.*, 2010; Sojka *et al.*, 2011; Todoshchenko *et al.*, 2014; Venezuela *et al.*, 2016; Wang *et al.*, 2018; Yang *et al.*, 2016, 2018; Zhu *et al.*, 2014). The plot includes data from dual phase, TRIP, martensitic, ferrite-bainite, high strength low alloy, complex phase, and TRIP aided bainitic ferrite grades, with tensile strength levels ranging from approximately 500 MPa to 1670 MPa. The figure shows a scattered but obvious correlation between tensile ductility loss and ultimate tensile strength. The correlation between tensile ductility loss and other tensile test measurements, e.g., yield strength, yield to tensile strength ratio, ductility in air, is not as strong. The scatter in the data is likely due to different testing parameters employed in the various laboratories. Variations in inclusion population could also lead to differences in performance as inclusions have been noted to be the source of crack nucleation in multiple studies (Bollinger *et al.*, 2019; Lee *et al.*, 2010; Sojka *et al.*, 2011). There is not a consistent correlation between the type of microstructure and its relative hydrogen embrittlement resistance. Todoshchenko *et al.* (2014) and the HydraMicros study (Hickel *et al.*, 2015) found that tempered martensite and dual phase ferrite-martensite microstructures are generally more resistant to hydrogen embrittlement than their non-tempered counterparts at a comparable strength level. However, these findings do not extend across studies as shown in **Fig. 5**. It should be noted that the amount of hydrogen absorption during the pre-charging portion of these experiments is usually greater than 1 ppm, far higher than the measured hydrogen absorption cited previously during steel production and typical service conditions.

Amongst the AHSS shown in **Fig. 5** and those used and considered for automotive application, several contain metastable retained austenite. As noted in the section on Hydrogen Gas Storage and Transportation, hydrogen has a low diffusivity of $2 \cdot 10^{-11}$ to $2 \cdot 10^{-13}$ cm$^2 \cdot$ s^{-1} in austenite (Olden *et al.*, 2014; Tsong-Pyng and Altstetter, 1986; Turnbull and Hutchings, 1994) compared to ferrite and martensite, where the hydrogen diffusivity is $1 \cdot 10^{-4}$ to $6.7 \cdot 10^{-9}$ cm$^2 \cdot$ s^{-1} (Hirth, 1980; Maroef *et al.*, 2002; Olden *et al.*, 2014; Turnbull and Hutchings, 1994). In contrast, the solubility of hydrogen in austenite is reported to be three orders of magnitude higher than it is in ferritic phases (Turnbull and Hutchings, 1994). Because of the relatively high solubility and low diffusivity, retained austenite may be an effective hydrogen trap site to reduce hydrogen in the lattice; retained austenite has a reported binding energy for hydrogen trapping of 55 kJ/mol (Park *et al.*, 2002). However, the retained austenite in AHSS is generally employed to promote work hardening through deformation induced transformation to martensite. Since austenite has a much higher solubility for hydrogen, deformation induced transformation to martensite could result in supersaturation of hydrogen in the martensite, which would likely be deleterious for hydrogen embrittlement. Thus, there are potentially competing mechanisms associated with the effect of retained austenite on hydrogen embrittlement. As **Fig. 5** shows, there is not a consistent correlation between the steels with retained austenite (TR, QP, TBF) and the hydrogen susceptibility compared to the other AHSS. In a subset of these data, Bollinger *et al.* (2019) found that increased retained austenite in TRIP aided bainitic ferrite steels promoted hydrogen embrittlement because of increased hydrogen absorption, as the retained austenite underwent deformation induced transformation to martensite during tensile testing. Similarly, Ronevich *et al.* (2010) showed that a TRIP780 steel had a larger ductility loss in hydrogen than a TRIP980 steel despite the lower strength level; the difference was postulated to be from the larger and less stable retained austenite in the TRIP780 steel.

Hydrogen induced damage in AHSS generally occurs within martensite present as a result of heat treatment or deformation induced phase transformation, or at the boundary between martensite and ferrite. Martensite is well-established to be the most susceptible microconstituent in steels to hydrogen embrittlement. Several authors have noted that cracks initiated within martensite or at martensite-ferrite phase boundaries propagate and arrest within less susceptible ferritic regions. In steels composed

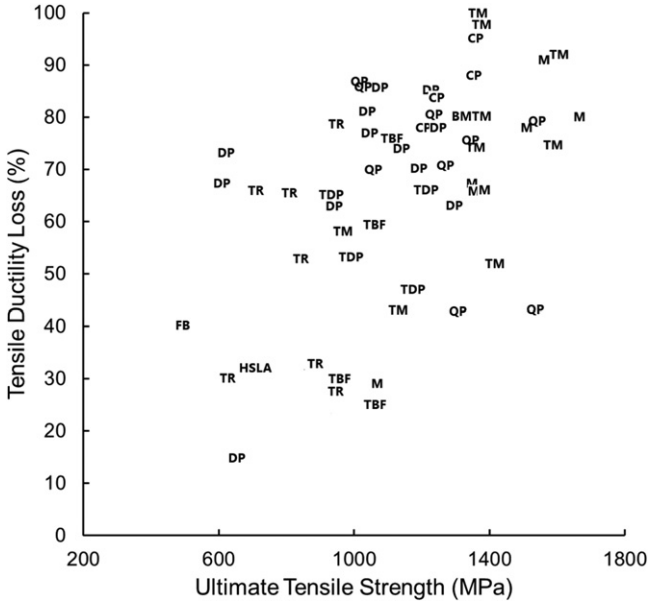

Fig. 5 Tensile ductility loss, referring to total elongation values, versus ultimate tensile strength for several AHSS grades (BMTM: Bainite-Martensite-Tempered Martensite, CP: Complex Phase, DP: Dual Phase, FB: Ferrite-Bainite, HSLA: High Strength, Low Alloy, M: Martensite, QP: Quenched and Partitioned, TBF: TRIP-aided Bainitic Ferrite, TDP: Tempered Dual Phase, TM: Tempered Martensite, TR: TRIP). These studies were all performed with hydrogen pre-charging utilizing H_2SO_4 solutions. Reproduced from Bollinger, A.L., Murakami, T., Findley, K.O., De Moor, E., Speer, J.G., 2019. The influence of microstructural variations on hydrogen absorbance and tensile properties at elevated hydrogen levels for TRIP-aided bainitic ferrite steels. Corrosion 75 (8), 888–897. Available at: https://doi.org/10.5006/3105. Depover, T., Pérez Escobar, D., Wallaert, E., Zermout, Z., Verbeken, K., 2014. Effect of hydrogen charging on the mechanical properties of advanced high strength steels. International Journal of Hydrogen Energy 39 (9), 4647–4656. Available at: https://doi.org/10.1016/j.ijhydene.2013.12.190. Hickel, T., Nazarov, R., McEniry, E., *et al.*, 2015. Hydrogen Sensitivity of Different Advanced High Strength Microstructures (HYDRAMICROS). Publications Office of the EU. Hilditch, T.B., Lee, S.B., Speer, J.G., Matlock, D.K., 2003. Response to hydrogen charging in high strength automotive sheet steel products. In: Proceedings of the SAE Technical Papers. doi:10.4271/2003-01-0525. Lee, S.J., Ronevich, J.A., Krauss, G., Matlock, D.K., 2010. Hydrogen embrittlement of hardened low-carbon sheet steel. ISIJ International 50 (2), 294–301. Available at: https://doi.org/10.2355/isijinternational.50.294. Liu, Q., Zhou, Q., Venezuela, J., Zhang, M., Atrens, A., 2017. Hydrogen influence on some advanced high-strength steels. Corrosion Science 125 (March), 114–138. Available at: https://doi.org/10.1016/j.corsci.2017.06.012. Ronevich, J.A., De Cooman, B.C., Speer, J.G., De Moor, E., Matlock, D.K., 2012. Hydrogen effects in prestrained transformation induced plasticity steel. Metallurgical and Materials Transactions A: Physical Metallurgy and Materials Science 43 (7), 2293–2301. Avalaible at: https://doi.org/10.1007/s11661-011-1075-3. Ronevich, J.A., Speer, J.G., Matlock, D.K., 2010. Hydrogen embrittlement of commercially produced advanced high strength sheet steels. SAE Technical Papers 255–267. Available at: https://doi.org/10.4271/2010-01-0447. Venezuela, J., Zhou, Q., Liu, Q., Zhang, M., Atrens, A., 2016. Influence of hydrogen on the mechanical and fracture properties of some martensitic advanced high strength steels in simulated service conditions. Corrosion Science 111, 602–624 Available at: https://doi.org/10.1016/j.corsci.2016.05.040. Wallaert, E., Depover, T., Arafin, M., Verbeken, K., 2014. Thermal desorption spectroscopy evaluation of the hydrogen-trapping capacity of NbC and NbN precipitates. Metallurgical and Materials Transactions A: Physical Metallurgy and Materials Science 45 (5), 2412–2420. Available at: https://doi.org/10.1007/s11661-013-2181-1. Wang, Z., Luo, Z.C., Huang, M.X., 2018. Revealing hydrogen-induced delayed fracture in ferrite-containing quenching and partitioning steels. Materialia 4 (September), 260–267. Available at: https://doi.org/10.1016/j.mtla.2018.09.022. Yang, J., Huang, F., Guo, Z., Rong, Y., Chen, N., 2016. Effect of retained austenite on the hydrogen embrittlement of a medium carbon quenching and partitioning steel with refined microstructure. Materials Science and Engineering A 665, 76–85. Available at: https://doi.org/10.1016/j.msea.2016.04.025. Yang, J., Song, Y., Lu, Y., Gu, J., Guo, Z., 2017. Effect of ferrite on the hydrogen embrittlement in quenched-partitioned-tempered low carbon steel. Materials Science and Engineering A 712 (July), 630–636. Available at: doi:10.1016/j.msea.2017.12.032.

entirely of martensite, as noted in the Section on High Strength Medium Carbon Steels for Fasteners, crack propagation is often intergranular, particularly at high strength levels. In multiphase steels, crack propagation has been observed to be both transgranular through ferritic regions or intergranular along phase boundaries (Bollinger *et al.*, 2019; Hickel *et al.*, 2015; Hilditch *et al.*, 2003; Liu *et al.*, 2016; Lovicu *et al.*, 2013; Ronevich *et al.*, 2012, 2010; Wang *et al.*, 2018; Yang *et al.*, 2018).

Summary and Opportunities for Future Research and Development Directions

This article has reviewed critical steel hydrogen embrittlement concepts in four product areas: high strength fasteners, austenitic stainless steels for hydrogen storage and transport, pipeline steels in sour service, and advanced high strength sheet steels for automotive applications.

The section on high strength fasteners reveals that microstructural design has enhanced the performance of martensitic steels in hydrogen environments through precipitates intended to trap hydrogen. Further opportunity exists for microstructural design and to evaluate the effectiveness of hydrogen traps and various microstructures in service conditions where the trapping effectiveness may vary compared to laboratory experiments. This relationship between laboratory and application results is an important theme that threads through all of the product areas in this article.

In hydrogen storage and distribution applications using austenitic stainless steel, the importance of hydrogen promoting localized deformation was discussed. This localized deformation affects fracture mechanisms and is controlled by austenite stacking fault energy and stability. The importance of the latter factor on overall hydrogen embrittlement resistance in these systems is still being explored. Fatigue and fatigue crack growth in hydrogen environments are similarly correlated to austenite strength and composition; however, there are conflicting reports on the role of hydrogen in increasing or decreasing fatigue lives. Thus, there is further opportunity to delineate the effect of hydrogen on both fatigue crack nucleation and growth behavior.

The section on pipeline steels for sour service summarized strategies employed to mitigate HIC, including inclusion and hard band control. However, the advantage of using higher strength levels in these applications justifies continued exploration of the role of other microstructural features such as microstructure texture, martensite-austenite constituents, and microstructures designed for hydrogen trapping.

The role of steel processing, component manufacturing, and product use on hydrogen pick up was presented in the section on advanced high strength steels in conjunction with testing methodologies associated with various aspects of performance. An assessment of ductility loss in hydrogen charged tensile specimens for a broad range of AHSS reveals that hydrogen susceptibility generally scales with strength, but there is an inconsistent correlation with microstructural aspects such as retained austenite. Some studies have indicated that hydrogen embrittlement resistance decreases as retained austenite stability decreases, though further work on the influence of austenite on hydrogen trapping and the role of austenite stability is necessary.

All of these research and development areas would benefit from further experimental and modeling efforts to establish accelerated test conditions that match service conditions. Often, laboratory tests are designed to be conducted with time efficiency as a high priority, which can result in a significant mismatch between laboratory and service conditions. For example, electrochemical charging often generates greater than 1 ppm of hydrogen in laboratory specimens, though studies on automotive steels indicate substantially less hydrogen pick up in manufacturing and service environments. Therefore, there are opportunities for the research and development and steel-using communities to partner to design tests to not only rank alloys with respect to hydrogen embrittlement but also provide relevant design metrics for steel product use.

References

Abraham, D.P., Altstetter, C.J., 1995. Hydrogen-enhanced localization of plasticity in an austenitic stainless steel. Metallurgical and Materials Transactions A 26 (11), 2859–2871. https://doi.org/10.1007/BF02669644.

Akiyama, E., 2012. Evaluation of delayed fracture property of high strength bolt steels. ISIJ International 52 (2), 307–315. https://doi.org/10.2355/isijinternational.52.307.

Amaro, R.L., Rustagi, N., Findley, K.O., Drexler, E.S., Slifka, A.J., 2014. Modeling the fatigue crack growth of X100 pipeline steel in gaseous hydrogen. International Journal of Fatigue 59. https://doi.org/10.1016/j.ijfatigue.2013.08.010.

Angus, G.R., Martins, G.P., Speer, J.G., Matlock, D.K., Findley, K.O., 2014. Characterization of an electrolytic charging method to assess hydrogen-induced damage in pipeline steels. In: Duprez, L., Zermout, Z. (Eds.), Steely Hydrogen. OCAS, pp. 291–302.

Aoki, Y., Kawamoto, K., Oda, Y., Noguchi, H., Higashida, K., 2005. Fatigue characteristics of a type 304 austenitic stainless steel in hydrogen gas environment. International Journal of Fracture 133 (3), 277–288. https://doi.org/10.1007/s10704-005-4942-3.

Asahi, H., Hirakami, D., Yamasaki, S., 2003a. Hydrogen trapping behavior in vanadium-added steel. ISIJ International 43 (4), 527–533. https://doi.org/10.2355/isijinternational.43.527.

Atrens, A., Liu, Q., Zhou, Q., Venezuela, J., Zhang, M., 2018. Evaluation of automobile service performance using laboratory testing. Materials Science and Technology 34 (15), 1893–1909. https://doi.org/10.1080/02670836.2018.1495903.

Banerjee, K., Chatterjee, U.K., 1999. Hydrogen embrittlement of a HSLA-100 steel in seawater. ISIJ International 39 (1), 47–55. https://doi.org/10.2355/isijinternational.39.47.

Barrera, O., Bombac, D., Chen, Y., *et al.*, 2018. Understanding and mitigating hydrogen embrittlement of steels: A review of experimental, modelling and design progress from atomistic to continuum. Journal of Materials Science 53 (9), 6251–6290. https://doi.org/10.1007/s10853-017-1978-5.

Beachem, C.D., 1972. A new model for hydrogen-assisted cracking (hydrogen "embrittlement"). Metallurgical Transactions 3 (2), 441–455. https://doi.org/10.1007/BF02642048.

Bergmann, C., Mraczek, K., Kroger, B., *et al.*, 2018. Hydrogen embrittlement resistance evaluation of advanced high strength steels in automotive applications. Duprez, L., Zermout, Z., Moli Sanchez, L., Van den Bergh, K. (Eds.), Proceedings - Steelyhydrogen, OCAS. (steelyhydrogen2021.be).

Bhadeshia, H.K.D.H., 2016. Prevention of hydrogen embrittlement in steels. ISIJ International 56 (1), 24–36. https://doi.org/10.2355/isijinternational.ISIJINT-2015-430.

Birnbaum, H.K., Sofronis, P., 1994. Hydrogen-enhanced localized plasticity – A mechanism for hydrogen-related fracture. Materials Science and Engineering A 176 (1–2), 191–202. https://doi.org/10.1016/0921-5093(94)90975-X.

Bollinger, A.L., Murakami, T., Findley, K.O., De Moor, E., Speer, J.G., 2019. The influence of microstructural variations on hydrogen absorbance and tensile properties at elevated hydrogen levels for TRIP-aided bainitic ferrite steels. Corrosion 75 (8), 888–897. https://doi.org/10.5006/3105.

Bott, A.H., Dos Santos, D.S., De Miranda, P.E.V., 1993. Influence of cementite morphology on the hydrogen permeation parameters of low-carbon steel. Journal of Materials Science Letters 12 (6), 390–393. https://doi.org/10.1007/BF00609163.

Brahimi, S.V., Yue, S., Sriraman, K.R., 2017. Alloy and composition dependence of hydrogen embrittlement susceptibility in high-strength steel fasteners. Philosophical Transactions of the Royal Society A: Mathematical, Physical and Engineering Sciences 375 (2098), https://doi.org/10.1098/rsta.2016.0407.

Brooks, J.A., West, A.J., Thompson, A.W., 1983. Effect of weld composition and microstructure on hydrogen assisted fracture of austenitic stainless steel. Metallurgical Transactions A 14A (1), 75–84. https://doi.org/10.1007/BF02643740.

Brown, A., Jones, C.L., 1984. Hydrogen induced cracking in pipeline steels. Corrosion 40 (7), 330–336. https://doi.org/10.5006/1.3593931.

Campbell, F.C., 2008. Stainless steels. In Elements of Metallurgy & Engineering Alloys. ASM International. pp. 433–451.

Caskey Jr., G.R., 1981. Hydrogen damage in stainless steels. In: Louthan, M.R., McNitt, R.P., Sisson, R.D. (Eds.), Environmental Degradation of Engineering Materials in Hydrogen. Virginia Polytechnic Institute, pp. 283–302.

Caskey Jr., G.R., 1983. Hydrogen Compatibility Handbook for Stainless Steels. Savannah River Laboratory Technical Report DP-1643. Aikin, SC.
Connolly, M., Martin, M., Bradley, P., *et al.*, 2019. In situ high energy X-ray diffraction measurement of strain and dislocation density ahead of crack tips grown in hydrogen. Acta Materialia 180, 272–286. https://doi.org/10.1016/j.actamat.2019.09.020.
Cornette, D., Allely, C., Dietsch, P., *et al.*, 2014. No detrimental impact of car manufacturing process and simulation of vehicle in-service conditions on DP1180 hydrogen embrittlement. In: Duprez, L., Zermout, Z. (Eds.), Steely Hydrogen. OCAS.
Dadfarnia, M., Sofronis, P., Neeraj, T., 2011. Hydrogen interaction with multiple traps: Can it be used to mitigate embrittlement? International Journal of Hydrogen Energy 36 (16), 10141–10148. https://doi.org/10.1016/j.ijhydene.2011.05.027.
Das, T., Rajagopalan, S.K., Brahimi, S.V., Wang, X., Yue, S., 2018. A study on the susceptibility of high strength tempered martensite steels to hydrogen embrittlement (HE) based on incremental step load (ISL) testing methodology. Materials Science and Engineering A 716, 189–207. https://doi.org/10.1016/j.msea.2018.01.032.
De Cooman, B.C., Speer, J.G., 2011. Fundamentals of Steel Product Physical Metallurgy. Association for Iron & Steel Technology.
Depover, T., Pérez Escobar, D., Wallaert, E., Zermout, Z., Verbeken, K., 2014. Effect of hydrogen charging on the mechanical properties of advanced high strength steels. International Journal of Hydrogen Energy 39 (9), 4647–4656. https://doi.org/10.1016/j.ijhydene.2013.12.190.
Díaz, A., Alegre, J.M., Cuesta, I.I., 2016. A review on diffusion modelling in hydrogen related failures of metals. Engineering Failure Analysis 66, 577–595. https://doi.org/10.1016/j.engfailanal.2016.05.019.
Doig, P., 1981. A model for the initiation of hydrogen embrittlement cracks at blunt notches during elastic fatigue loading. Materials Science and Engineering 48 (2), 181–188. https://doi.org/10.1016/0025-5416(81)90003-3.
Domizzi, G., Anteri, G., Ovejero-García, J., 2001. Influence of sulphur content and inclusion distribution on the hydrogen induced blister cracking in pressure vessel and pipeline steels. Corrosion Science 43 (2), 325–339. https://doi.org/10.1016/S0010-938X(00)00084-6.
Dong, C.F., Li, X.G., Liu, Z.Y., Zhang, Y.R., 2009. Hydrogen-induced cracking and healing behaviour of X70 steel. Journal of Alloys and Compounds 484 (1–2), 966–972. https://doi.org/10.1016/j.jallcom.2009.05.085.
Ferreira, P.J., Robertson, I.M., Birnbaum, H.K., 1999. Hydrogen effects on the character of dislocations in high-purity aluminum. Acta Materialia 47 (10), 2991–2998. https://doi.org/10.1016/S1359-6454(99)00156-1.
Findley, K.O., O'Brien, M.K., Nako, H., 2015. Critical assessment 17: Mechanisms of hydrogen induced cracking in pipeline steels. Materials Science and Technology 31 (14), 1673–1680. https://doi.org/10.1080/02670836.2015.1121017.
Fukuyama, S., Yokogawa, K., Kudo, K., Araki, M., 1985. Fatigue properties of Type 304 stainless steel in high pressure hydrogen at room temperature. Transactions of the Japan Institute of Metals 26, 325–331.
Fukuyama, S., Imade, M., Lin, Z., Yokogawa, K., 2005. Hydrogen embrittlement of metals in 70 MPa hydrogen at room temperature. In: ASME (Ed.), Proceedings of Pressure Vessels and Piping Conference., pp. 493–497.
Gangloff, R.P., 2003. Hydrogen assisted cracking of high strength alloys. Comprehensive Structural Integrity. 31–101.
Gangloff, R.P., Wei, R.P., 1978. Fractographic analysis of gaseous hydrogen induced cracking in 18Ni maraging steel. In: Strauss, B., Cullen, W. (Eds.), Fractography in Failure Analysis. West Conshohocken, PA: ASTM International, pp. 87–106. https://doi.org/10.1520/stp38087s.
Garrison, W.M., Moody, N.R., 2012. Hydrogen embrittlement of high strength steels. In: Gangloff, R., Somerday, B. (Eds.), Gaseous Hydrogen Embrittlement of Materials in Energy Technologies: The Problem, its Characterisation and Effects on Particular Alloy Classes. Woodhead Publishing, pp. 421–492.
Gibbs, P.J., Hough, P.D., Thürmer, K., *et al.*, 2020. Stacking fault energy based alloy screening for hydrogen compatibility. JOM 72 (5), 1982–1992. https://doi.org/10.1007/s11837-020-04106-7.
Gibbs, P.J., Marchi, C.S., Nibur, K.A., Tang, X., 2016. Comparison of internal and external hydrogen on fatigue-life of austenitic stainless steels. In: Proceedings of the Pressure Vessels and Piping Division (Publication) PVP, 6B-2016. American Society of Mechanical Engineers. doi: 10.1115/PVP2016-63563.
Han, G., He, J., Fukuyama, S., Yokogawa, K., 1998. Effect of strain-induced martensite on hydrogen environment embrittlement of sensitized austenitic stainless steels at low temperatures. Acta Materialia 46 (13), 4559–4570.
Hanninen, H.E., 1979. Influence of metallurgical variables on environment-sensitive cracking of austenitic alloys. International Metals Reviews 24 (1), 85–136.
Hay, M.G., 2001. Fitness-for-purpose material testing for sour gas service – An overview. Corrosion 57 (3), 236–252. https://doi.org/10.5006/1.3290348.
Hickel, T., Nazarov, R., McEniry, E., *et al.*, 2015. Hydrogen Sensitivity of Different Advanced High Strength Microstructures (HYDRAMICROS). Publications Office of the EU.
Hilditch, T.B., Lee, S.B., Speer, J.G., Matlock, D.K., 2003. Response to hydrogen charging in high strength automotive sheet steel products. In: Proceedings of the SAE Technical Papers. doi: 10.4271/2003-01-0525.
Hirth, J.P., 1980. Effects of hydrogen on the properties of iron and steel. Metallurgical Transactions A 11 (6), 861–890. https://doi.org/10.1007/BF02654700.
Hong, G.W., Lee, J.Y., 1983a. The measurement of the trap binding energy by the thermal analysis technique. Scripta Metallurgica 17 (7), 823–826. https://doi.org/10.1016/0036-9748(83)90242-9.
Hong, G.W., Lee, J.Y., 1983b. The interaction of hydrogen with iron oxide inclusions in iron. Materials Science and Engineering 61 (3), 219–225. https://doi.org/10.1016/0025-5416(83)90103-9.
Huang, F., Li, X.G., Liu, J., *et al.*, 2011. Hydrogen-induced cracking susceptibility and hydrogen trapping efficiency of different microstructure X80 pipeline steel. Journal of Materials Science 46 (3), 715–722. https://doi.org/10.1007/s10853-010-4799-3.
Huang, F., Cheng, P., Zhao, X.Y., *et al.*, 2017. Effect of sulfide films formed on X65 steel surface on hydrogen permeation in H2S environments. International Journal of Hydrogen Energy 42 (7), 4561–4570. https://doi.org/10.1016/j.ijhydene.2016.10.130.
Hui, W., Zhang, Y., Zhao, X., *et al.*, 2016. Influence of cold deformation and annealing on hydrogen embrittlement of cold hardening bainitic steel for high strength bolts. Materials Science and Engineering A 662, 528–536. https://doi.org/10.1016/j.msea.2016.03.104.
Hyer-Peterson, D., 2019. Hydrogen Embrittlement of 4340 with Martensitic and Bainitic Microstructures for Fastener Applications. (M.S. thesis). Colorado School of Mines.
Inagaki, H., Tanimura, M., Matsushima, I., Nishimura, T., 1978. Effect of Cu on the hydrogen induced cracking of the pipe line steel. Transactions of the Iron and Steel Institute of Japan 18 (3), 149–156. https://doi.org/10.2355/isijinternational1966.18.149.
Johnson, T., Benard, P., 2016. Solid-state H_2 storage system engineering: Direct H_2 refueling. In Hydrogen Storage Technology: Materials and Applications. pp. 347–384.
Johnson, W.H., 1875. On some remarkable changes produced in iron and steel by the action of hydrogen and acids. Nature 11 (281), 393. https://doi.org/10.1038/011393a0.
Kanezaki, T., Narazaki, C., Mine, Y., Matsuoka, S., Murakami, Y., 2008. Effects of hydrogen on fatigue crack growth behavior of austenitic stainless steels. International Journal of Hydrogen Energy 33, 2604–2619.
Kanezaki, T., Mine, Y., Fukushima, Y., Murakami, Y., 2004. Effects of hydrogen on fatigue crack growth behaviour and ductility loss of austenitic stainless steels. In: Proceedings of the ECF15.
Kim, W.K., Koh, S.U., Yang, B.Y., Kim, K.Y., 2008b. Effect of environmental and metallurgical factors on hydrogen induced cracking of HSLA steels. Corrosion Science 50 (12), 3336–3342. https://doi.org/10.1016/j.corsci.2008.09.030.
Koyama, M., Tasan, C.C., Akiyama, E., Tsuzaki, K., Raabe, D., 2014. Hydrogen-assisted decohesion and localized plasticity in dual-phase steel. Acta Materialia 70, 174–187. https://doi.org/10.1016/j.actamat.2014.01.048.
Krauss, G., 2011. Martensitic microstructural systems in carbon steels and susceptibility to hydrogen embrittlement. Iron and Steel Technology 8 (9), 187–195.
Krauss, G., 2015. Steels: Processing, Structure, and Performance, second ed. ASM International.
Krom, A.H.M., Bakker, A.D., 2000. Hydrogen trapping models in steel. Metallurgical and Materials Transactions B: Process Metallurgy and Materials Processing Science 31 (6), 1475–1482. https://doi.org/10.1007/s11663-000-0032-0.

Krom, A.H.M., Bakker, A., Koers, R.W.J., 1997. Modelling hydrogen-induced cracking in steel using a coupled diffusion stress finite element analysis. International Journal of Pressure Vessels and Piping 72 (2), 139–147. https://doi.org/10.1016/S0308-0161(97)00019-7.
Lee, H.G., Lee, J.Y., 1984. Hydrogen trapping by TiC particles in iron. Acta Metallurgica 32 (1), 131–136. https://doi.org/10.1016/0001-6160(84)90210-4.
Lee, J., Lee, T., Kwon, Y.J., *et al.*, 2016. Effects of vanadium carbides on hydrogen embrittlement of tempered martensitic steel. Metals and Materials International 22 (3), 364–372. https://doi.org/10.1007/s12540-016-5631-7.
Lee, S.J., Ronevich, J.A., Krauss, G., Matlock, D.K., 2010. Hydrogen embrittlement of hardened low-carbon sheet steel. ISIJ International 50 (2), 294–301. https://doi.org/10.2355/isijinternational.50.294.
Liang, Y., Sofronis, P., Aravas, N., 2003. On the effect of hydrogen on plastic instabilities in metals. Acta Materialia 51 (9), 2717–2730. https://doi.org/10.1016/S1359-6454(03)00081-8.
Liou, H.Y., Shieh, R.I., Wei, F.I., Wang, S.C., 1993. Roles of microalloying elements in hydrogen induced cracking resistant property HSLA steel. Corrosion 49 (5), 389–398. https://doi.org/10.5006/1.3316066.
Liu, Q., Zhou, Q., Venezuela, J., Zhang, M., Atrens, A., 2016. Hydrogen concentration in dual-phase (DP) and quenched and partitioned (Q&P) advanced high-strength steels (AHSS) under simulated service conditions compared with cathodic charging conditions. Advanced Engineering Materials 18 (9), 1588–1599. https://doi.org/10.1002/adem.201600217.
Liu, Q., Zhou, Q., Venezuela, J., Zhang, M., Atrens, A., 2017. Hydrogen influence on some advanced high-strength steels. Corrosion Science 125 (March), 114–138. https://doi.org/10.1016/j.corsci.2017.06.012.
Lo, K.H., Shek, C.H., Lai, J.K.L., 2009. Recent developments in stainless steels. Materials Science and Engineering R: Reports 65, 39–104.
Lovicu, G., Paravicini Bagliani, E., De Sanctis, M., *et al.*, 2013. Hydrogen embrittlement of a medium carbon Q&P steel. Metallurgia Italiana 105 (6), 3–10.
Lynch, S.P., 1988. Environmentally assisted cracking: overview of evidence for an adsorption-induced localised-slip process. Acta Metallurgica 36 (10), 2639–2661. https://doi.org/10.1016/0001-6160(88)90113-7.
Maroef, I., Olson, D.L., Eberhart, M., Edwards, G.R., 2002. Hydrogen trapping in ferritic steel weld metal. International Materials Reviews 47 (4), 191–223. https://doi.org/10.1179/095066002225006548.
Martin, M.L., Dadfarnia, M., Nagao, A., Wang, S., Sofronis, P., 2019. Enumeration of the hydrogen-enhanced localized plasticity mechanism for hydrogen embrittlement in structural materials. Acta Materialia 165, 734–750. https://doi.org/10.1016/j.actamat.2018.12.014.
Matsumoto, K., Kobayashi, Y., Ume, K., *et al.*, 1986. Hydrogen induced cracking susceptibility of high-strength line pipe steels. Corrosion 42 (6), 337–345. https://doi.org/10.5006/1.3584913.
McCarty, E.D., Wetzel, D., Kloberdanz, B.S., 1996. Hydrogen embrittlement in automotive fastener applications. Journal of Materials & Manufacturing 105, 355–383.
McMahon, C., 2012. The role of grain boundaries in hydrogen induced cracking (HIC) of steels. In: Gangloff, P., Somerday, B.P. (Eds.), Gaseous Hydrogen Embrittlement of Materials in Energy Technologies: Mechanisms, Modeling, and Future Developments. Woodhead Publishing, pp. 154–165.
McMahon, C.J., 2001. Hydrogen-induced intergranular fracture of steels. Engineering Fracture Mechanics 68 (6), 773–788. https://doi.org/10.1016/S0013-7944(00)00124-7.
Michler, T., Naumann, J., 2010. Microstructural aspects upon hydrogen environment embrittlement of various bcc steels. International Journal of Hydrogen Energy 35 (2), 821–832. https://doi.org/10.1016/j.ijhydene.2009.10.092.
Michler, T., Naumann, J., Sattler, E., 2013a. Influence of high pressure gaseous hydrogen on S-N fatigue in two austenitic stainless steels. International Journal of Fatigue 51, 1–7. https://doi.org/10.1016/j.ijfatigue.2013.01.010.
Michler, T., Naumann, J., Weber, S., Martin, M., Pargeter, R., 2013b. S-N fatigue properties of a stable high-aluminum austenitic stainless steel for hydrogen applications. International Journal of Hydrogen Energy 38 (23), 9935–9941. https://doi.org/10.1016/j.ijhydene.2013.05.145.
Michler, T., Lee, Y., Gangloff, R.P., Naumann, J., 2009. Influence of macro segregation on hydrogen environment embrittlement of SUS 316L stainless steel. International Journal of Hydrogen Energy 34 (7), 3201–3209.
Mohtadi-Bonab, M.A., Eskandari, M., Szpunar, J.A., 2016. Effect of arisen dislocation density and texture components during cold rolling and annealing treatments on hydrogen induced cracking susceptibility in pipeline steel. Journal of Materials Research 31 (21), 3390–3400. https://doi.org/10.1557/jmr.2016.357.
Mohtadi-Bonab, M.A., Szpunar, J.A., Basu, R., Eskandari, M., 2015. The mechanism of failure by hydrogen induced cracking in an acidic environment for API 5L X70 pipeline steel. International Journal of Hydrogen Energy 40 (2), 1096–1107. https://doi.org/10.1016/j.ijhydene.2014.11.057.
Moody, N.R., Robinson, S.L., Garrison, W.M., 1990. Hydrogen effects on the properties and fracture modes of iron-based alloys. Res Mechanica 30, 143–206.
Murakami, Y., Matsunaga, H., 2006. The effect of hydrogen on fatigue properties of steels used for fuel cell system. International Journal of Fatigue 28 (11), 1509–1520. https://doi.org/10.1016/j.ijfatigue.2005.06.059.
Murakami, Y., Kanezaki, T., Mine, Y., 2010. Hydrogen effect against hydrogen embrittlement. Metallurgical and Materials Transactions A 41, 2548–2562.
NACE International. (2003). NACE MR0175/ISO15156-2, 'Petroleum and Natural Gas Industries - Materials for Use in H2S Containing Environments in Oil and Gas Production - Part 2: Cracking-Resistant Carbon and Low Alloy Steel, and the Use of Cast Iron.
Nagao, A., Martin, M.L., Dadfarnia, M., Sofronis, P., Robertson, I.M., 2014. The effect of nanosized (Ti,Mo)C precipitates on hydrogen embrittlement of tempered lath martensitic steel. Acta Materialia 74, 244–254. https://doi.org/10.1016/j.actamat.2014.04.051.
Nagumo, M., Shimura, H., Chaya, T., Hayashi, H., Ochiai, I., 2003. Fatigue damage and its interaction with hydrogen in martensitic steels. Materials Science and Engineering A 348 (1–2), 192–200. https://doi.org/10.1016/S0921-5093(02)00745-1.
Nanninga, N., Grochowsi, J., Heldt, L., Rundman, K., 2010. Role of microstructure, composition and hardness in resisting hydrogen embrittlement of fastener grade steels. Corrosion Science 52 (4), 1237–1246. https://doi.org/10.1016/j.corsci.2009.12.020.
National Academy of Engineering, 2018. High-Performance Bolting Technology for Offshore Oil and Natural Gas Operations. National Academies Press. https://doi.org/10.17226/25032.
Nelson, H.G., 1983. Hydrogen embrittlement. Treatise on Materials Science and Technology 25, 275–359.
Nibur, K.A., Bahr, D.F., Somerday, B.P., 2006. Hydrogen effects on dislocation activity in austenitic stainless steel. Acta Materialia 54 (10), 2677–2684. https://doi.org/10.1016/j.actamat.2006.02.007.
Nibur, K.A., Somerday, B.P., Balch, D.K., San Marchi, C., 2009. The role of localized deformation in hydrogen-assisted crack propagation in 21Cr–6Ni–9Mn stainless steel. Acta Materialia 57 (13), 3795–3809.
Nibur, K.A., Gibbs, P.J., Foulk, J.W., San Marchi, C., 2017. Notched fatigue of austenitic alloys in gaseous hydrogen. In: Proceedings of the ASME Pressure Vessels and Piping Conference. pp. 459–465.
Nieto, J., Elías, T., Lopez, G., *et al.*, 2013. Effective process design for the production of HIC-resistant linepipe steels. Journal of Materials Engineering and Performance 22 (9), 2493–2499. https://doi.org/10.1007/s11665-013-0544-9.
Novak, P., Yuan, R., Somerday, B.P., Sofronis, P., Ritchie, R.O., 2010. A statistical, physical-based, micro-mechanical model of hydrogen-induced intergranular fracture in steel. Journal of the Mechanics and Physics of Solids 58 (2), 206–226. https://doi.org/10.1016/j.jmps.2009.10.005.
O'Brien, M.K., Findley, K.O., Speer, J.G., 2018. Effect of microstructure on hydrogen induced cracking in sour service pipeline steel. In: Proceedings of the 2nd International Symposium on the Recent Developments in Plate Steels. pp. 297–308.
Ohmiya, S., Fujii, H., 2007. Mechanical properties of cold worked type 316L stainless steel in high pressure gaseous hydrogen: Investigation of materials properties in high pressure gaseous hydrogen—3. In: Proceedings of the ASM Pressure Vessels and Piping Conference. pp. 459–465.
Ohmiya, S., Fujii, H., 2012. Effects of Ni and Cr contents on fatigue crack growth properties of SUS316-based stainless steels in high-pressure gaseous hydrogen. ISIJ International 52 (2), 247–254.

Olden, V., Saai, A., Jemblie, L., Johnsen, R., 2014. FE simulation of hydrogen diffusion in duplex stainless steel. International Journal of Hydrogen Energy 39 (2), 1156–1163. https://doi.org/10.1016/j.ijhydene.2013.10.101.
Olson, G.B., Cohen, M., 1975. Kinetics of strain-induced martensitic nucleation. Metallurgical Transactions A 6 (4), 791–795.
Omura, T., Miyahara, M., Semba, H., Igarashi, M., Hirata, H., 2007. Evaluation of hydrogen environment embrittlement and fatigue properties of stainless steels in high pressure gaseous hydrogen: Investigation of materials properties in high pressure gaseous hydrogen—2. In: Proceedings of Pressure Vessels and Piping Conference. pp. 467–474.
Ootsuka, S., Fujita, S., Tada, E., Nishikata, A., Tsuru, T., 2015. Evaluation of hydrogen absorption into steel in automobile moving environments. Corrosion Science 98, 430–437. https://doi.org/10.1016/j.corsci.2015.05.049.
Oriani, R.A., 1978. Hydrogen embrittlement of steels. Annual Review of Materials Science 8 (1), 327–357. https://doi.org/10.1146/annurev.ms.08.080178.001551.
Park, G.T., Koh, S.U., Jung, H.G., Kim, K.Y., 2008. Effect of microstructure on the hydrogen trapping efficiency and hydrogen induced cracking of linepipe steel. Corrosion Science 50 (7), 1865–1871. https://doi.org/10.1016/j.corsci.2008.03.007.
Park, Y.D., Maroef, I.S., Landau, A., Olson, D.L., 2002. Retained austenite as a hydrogen trap in steel welds. Welding Journal 81, 27S–35S.
Perra, M.W., Stoltz, R.E., 1980. Sustained-load cracking of a precipitation-strengthened austenitic steel in high-pressure hydrogen. In: Bernstein, I.M., Thompson, A.W. (Eds.), Hydrogen Effects in Metals, Proceedings of the Third International Conference on Effect of Hydrogen on Behavior of Materials. The Metallurgical Society of AIME, pp. 645–653.
Pressouyre, G.M., Bernstein, I.M., 1978. A quantitative analysis of hydrogen trapping. Metallurgical Transactions A 9 (11), 1571–1580. https://doi.org/10.1007/BF02661939.
Rath, B.B., Bernstein, I.M., 1971. The relation between grain-boundary orientation and intergranular cracking. Metallurgical Transactions 2 (10), 2845–2851. https://doi.org/10.1007/BF02813262.
Rehrl, J., Mraczek, K., Pichler, A., Werner, E., 2014a. Mechanical properties and fracture behavior of hydrogen charged AHSS/UHSS grades at high- and low strain rate tests. Materials Science and Engineering A 590, 360–367. https://doi.org/10.1016/j.msea.2013.10.044.
Rehrl, J., Mraczek, K., Pichler, A., Werner, E., 2014b. The impact of hydrogen on the mechanical properties of AHSS/UHSS grades at low- and high strain rates. In: Duprez, L., Zermout, Z. (Eds.), Steely Hydrogen. OCAS, pp. 291–302.
Revie, R.W., Sastri, V.S., Hoey, G.R., *et al.*, 1993. Hydrogen-induced cracking of linepipe steels part 1-threshold hydrogen concentration and pH. Corrosion 49 (1), 17–23. https://doi.org/10.5006/1.3316028.
Robertson, I.M., 2001. The effect of hydrogen on dislocation dynamics. Engineering Fracture Mechanics 68 (6), 671–692. https://doi.org/10.1016/S0013-7944(01)00011-X.
Robertson, I.M., Sofronis, P., Nagao, A., *et al.*, 2015. Hydrogen embrittlement understood. Metallurgical and Materials Transactions A: Physical Metallurgy and Materials Science 46 (6), 2323–2341. https://doi.org/10.1007/s11661-015-2836-1.
Ronevich, J.A., Speer, J.G., Matlock, D.K., 2010. Hydrogen embrittlement of commercially produced advanced high strength sheet steels. SAE Technical Papers. 255–267. https://doi.org/10.4271/2010-01-0447.
Ronevich, J.A., De Cooman, B.C., Speer, J.G., De Moor, E., Matlock, D.K., 2012. Hydrogen effects in prestrained transformation induced plasticity steel. Metallurgical and Materials Transactions A: Physical Metallurgy and Materials Science 43 (7), 2293–2301. https://doi.org/10.1007/s11661-011-1075-3.
San Marchi, C., 2012. Gaseous HE of materials in energy technologies. In: Gangloff, R.P., Somerday, B.P. (Eds.), Gaseous Hydrogen Embrittlement for Materials in Energy Technologies: The Problem, its Characterisation and Effects on Particular Alloys Classes. Woodhead Publishing, pp. 592–623.
San Marchi, C., Somerday, B.P., 2011. Fatigue crack growth of structural metals for hydrogen service. American Society of Mechanical Engineers, Pressure Vessels and Piping Division, PVP 6 (PARTS A AND B), 851–857. https://doi.org/10.1115/PVP2011-57701.
San Marchi, C., Somerday, B.P., Nibur, K.A., 2012. Fatigue crack initiation in hydrogen-precharged austenitic stainless steel. In: Proceedings of the 2008 International Hydrogen Conference. pp. 365–374.
San Marchi, C., Balch, D.K., Nibur, K., Somerday, B.P., 2008a. Effect of high-pressure hydrogen gas on fracture of austenitic steels. Journal of Pressure Vessel Technology 130 (4).
San Marchi, C., Somerday, B.P., Tang, X., Schiroky, G.H., 2008b. Effects of alloy composition and strain hardening on tensile fracture of hydrogen-precharged type 316 stainless steels. International Journal of Hydrogen Energy 33 (2), 889–904.
Skipper, C., Leisk, G., Saigal, A., Matson, D., San Marchi, C., 2008. Proceedings of the 2008 International Hydrogen Conference. pp. 139–146.
Sofronis, P., Liang, Y., Aravas, N., 2001. Hydrogen induced shear localization of the plastic flow in metals and alloys. European Journal of Mechanics, A/Solids 20 (6), 857–872. https://doi.org/10.1016/S0997-7538(01)01179-2.
Sojka, J., Vodárek, V., Schindler, I., *et al.*, 2011. Effect of hydrogen on the properties and fracture characteristics of TRIP 800 steels. Corrosion Science 53 (8), 2575–2581. https://doi.org/10.1016/j.corsci.2011.04.015.
Somerday, B.P., Dadfarnia, M., Balch, D.K., *et al.*, 2009. Hydrogen-assisted crack propagation in austenitic stainless steel fusion welds. Metallurgical and Materials Transactions A 40 (10), 2350–2362.
Stevens, M.F., Bernstein, I.M., 1989. Microstructural trapping effects on hydrogen induced cracking of a microalloyed steel. Metallurgical Transactions A 20 (5), 909–919. https://doi.org/10.1007/BF02651657.
Talonen, J., Hänninen, H., 2007. Formation of shear bands and strain-induced martensite during plastic deformation of metastable austenitic stainless steels. Acta Materialia 55 (18), 6108–6118. https://doi.org/10.1016/j.actamat.2007.07.015.
Tartaglia, J.M., Lazzari, K.A., Hui, G.P., Hayrynen, K.L., 2008. A comparison of mechanical properties and hydrogen embrittlement resistance of austempered vs quenched and tempered 4340 steel. Metallurgical and Materials Transactions A: Physical Metallurgy and Materials Science A 39, 559–576. https://doi.org/10.1007/s11661-007-9451-8.
Tetelman, A.S., Robertson, W.D., 1963. Direct observation and analysis of crack propagation in iron-3% silicon single crystals. Acta Metallurgica 11 (5), 415–426. https://doi.org/10.1016/0001-6160(63)90166-4.
Thompson, A.W., Buck, O., 1976. Hydrogen effects on martensite formation. Metallurgical Transactions A 7 (2), 329–331.
Todoshchenko, O., Yagodzinskyy, Y., Saukkonen, T., Hanninen, H., 2014. Hydrogen-induced delayed fracture of high-strength carbon steels. In: Duprez, L., Zermout, Z. (Eds.), Steely Hydrogen. OCAS, pp. 583–588.
Tsong-Pyng, P., Altstetter, C.J., 1986. Effects of deformation on hydrogen permeation in austenitic stainless steels. Acta Metallurgica 34 (9), 1771–1781. https://doi.org/10.1016/0001-6160(86)90123-9.
Turnbull, A., 2015. Perspectives on hydrogen uptake, diffusion and trapping. International Journal of Hydrogen Energy 40 (47), 16961–16970. https://doi.org/10.1016/j.ijhydene.2015.06.147.
Turnbull, A., Hutchings, R.B., 1994. Analysis of hydrogen atom transport in a two-phase alloy. Materials Science and Engineering 177, 161–171.
Ulmer, D.G., Altstetter, C.J., 1991. Hydrogen-induced strain localization and failure of austenitic stainless steels at high hydrogen concentrations. Acta Metallurgica Et Materialia 39 (6), 1237–1248. https://doi.org/10.1016/0956-7151(91)90211-I.
Venegas, V., Caleyo, F., Baudin, T., Espina-Hernández, J.H., Hallen, J.M., 2011. On the role of crystallographic texture in mitigating hydrogen-induced cracking in pipeline steels. Corrosion Science 53 (12), 4204–4212. https://doi.org/10.1016/j.corsci.2011.08.031.
Venezuela, J., Zhou, Q., Liu, Q., Zhang, M., Atrens, A., 2016. Influence of hydrogen on the mechanical and fracture properties of some martensitic advanced high strength steels in simulated service conditions. Corrosion Science 111, 602–624. https://doi.org/10.1016/j.corsci.2016.05.040.
Villalobos, J., Del-Pozo, A., Campillo, B., Mayen, J., Serna, S., 2018. Microalloyed steels through history until 2018: Review of chemical composition, processing and hydrogen service. Metals 8 (5), 351. https://doi.org/10.3390/met8050351.
Wang, M., Tasan, C.C., Koyama, M., Ponge, D., Raabe, D., 2015. Enhancing hydrogen embrittlement resistance of lath martensite by introducing nano-films of interlath austenite. Metallurgical and Materials Transactions A: Physical Metallurgy and Materials Science 46 (9), 3797–3802. https://doi.org/10.1007/s11661-015-3009-y.

Wang, W., Shan, Y., Yang, K., 2009. Study of high strength pipeline steels with different microstructures. Materials Science and Engineering A 502 (1–2), 38–44. https://doi.org/10.1016/j.msea.2008.10.042.
Wang, Z., Luo, Z.C., Huang, M.X., 2018. Revealing hydrogen-induced delayed fracture in ferrite-containing quenching and partitioning steels. Materialia 4 (September), 260–267. https://doi.org/10.1016/j.mtla.2018.09.022.
Wei, F.-G., Tsuzaki, K., 2008. Hydrogen trapping character of nano-sized NbC precipitates in tempered martensite. In: Somerday, B., Sofronis, P., Jones, R. (Eds.), Effects of Hydrogen on Materials; Proceedings of the 2008 International Hydrogen Conference., pp. 456–463.
Wei, F.-G., Hara, T., Tsuzaki, K., 2011. Nano-precipitates design with hydrogen trapping character in high strength steel. In Advanced Steels. Berlin Heidelberg: Springer, pp. 87–92. [10.1007/978-3-642-17665-4_11].
Wei, F.-G., Hara, T., Tsuchida, T., Tsuzaki, K., 2003. Hydrogen trapping in quenched and tempered 0.42C-0.30Ti steel containing bimodally dispersed TiC particles. ISIJ International 43 (4), 539–547. https://doi.org/10.2355/isijinternational.43.539.
Yang, J., Huang, F., Guo, Z., Rong, Y., Chen, N., 2016. Effect of retained austenite on the hydrogen embrittlement of a medium carbon quenching and partitioning steel with refined microstructure. Materials Science and Engineering A 665, 76–85. https://doi.org/10.1016/j.msea.2016.04.025.
Yang, J., Song, Y., Lu, Y., Gu, J., Guo, Z., 2018. Effect of ferrite on the hydrogen embrittlement in quenched-partitioned-tempered low carbon steel. Materials Science and Engineering A 712 (July 2017), 630–636. https://doi.org/10.1016/j.msea.2017.12.032.
Yu, G.H., Cheng, Y.H., Chen, L., *et al*., 1997. Hydrogen accumulation and hydrogen-induced cracking of API C90 tubular steel. Corrosion 53 (10), 762–769. https://doi.org/10.5006/1.3290260.
Zakroczymski, T., 1985. Permeability of iron to hydrogen cathodically generated in 0.1 M NaoH. Scripta Metallurgica 19 (4), 521–524. https://doi.org/10.1016/0036-9748(85)90126-7.
Zappfe, C.A., Sims, C.E., 1941. Hydrogen embrittlement, internal stress and defects in steel. Transactions of AIME 145, 225–271.
Zhang, L., Wen, M., Imade, M., Fukuyama, S., Yokogawa, K., 2008. Effect of nickel equivalent on hydrogen gas embrittlement of austenitic stainless steels based on type 316 at low temperatures. Acta Materialia 56 (3414–3421),
Zhu, X., Li, W., Zhao, H., Wang, L., Jin, X., 2014. Hydrogen trapping sites and hydrogen-induced cracking in high strength quenching & partitioning (Q&P) treated steel. International Journal of Hydrogen Energy 39 (24), 13031–13040. https://doi.org/10.1016/j.ijhydene.2014.06.079.